



<http://www.diva-portal.org>

Preprint

This is the submitted version of a paper published in *Microporous and Mesoporous Materials*.

Citation for the original published paper (version of record):

Klechikov, A., Sun, J., Hu, G., Zheng, M., Wågberg, T. et al. (2017)

Graphene decorated with metal nanoparticles: Hydrogen sorption and related artefacts.

*Microporous and Mesoporous Materials*, 250: 27-34

<https://doi.org/10.1016/j.micromeso.2017.05.014>

Access to the published version may require subscription.

N.B. When citing this work, cite the original published paper.

Permanent link to this version:

<http://urn.kb.se/resolve?urn=urn:nbn:se:umu:diva-135589>

# Graphene decorated with metal nanoparticles: hydrogen sorption and related artefacts.

Alexey Klechikov,<sup>1</sup> Jinhua Sun,<sup>1</sup> Guangzhi Hu,<sup>1</sup> Mingbo Zheng,<sup>2</sup> Thomas Wågberg,<sup>1</sup>  
Alexandr V.Talyzin<sup>1\*</sup>

<sup>1</sup>Department of Physics, Umeå University, S-90187 Umeå, Sweden

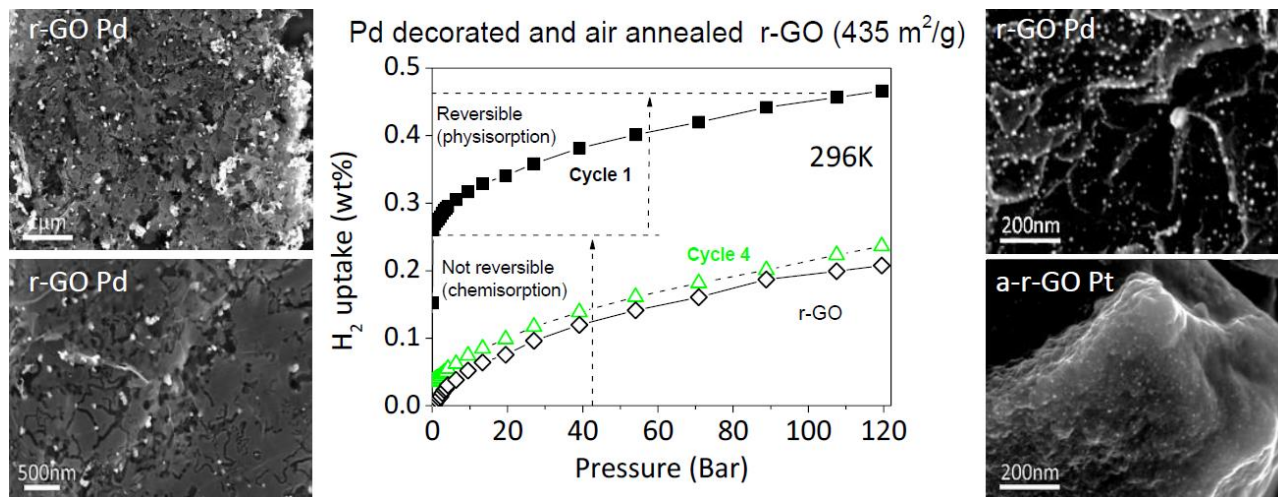
<sup>2</sup>College of Chemistry and Chemical Engineering, Yangzhou University, Yangzhou  
225002, China

\*Corresponding author

E-mail address: alexandr.talyzin@umu.se (A.V. Talyzin).

## ABSTRACT

Hydrogen sorption by reduced graphene oxides (r-GO) is not found to increase after decoration with Pd and Pt nanoparticles. Treatments of metal decorated samples using annealing under hydrogen or air were tested as a method to create additional pores by effects of r-GO etching around nanoparticles. Increase of Specific Surface Area (SSA) was observed for some air annealed r-GO samples. However, the same treatments applied to activated r-GO samples with microporous nature and higher surface area result in breakup of structure and dramatic decrease of SSA. Our experiments have not revealed effects which could be attributed to spillover in hydrogen sorption on Pd or Pt decorated graphene. However, we report irreversible chemisorption of hydrogen for some samples which can be mistakenly assigned to spillover if the experiments are incomplete.



KEYWORDS: graphene, hydrogen storage, graphene oxide, nanoparticles, decoration

## 1. Introduction

Storage of hydrogen remains to be the main obstacle in the development of hydrogen technology. Broad range of porous materials have been studied over past decades for hydrogen storage applications, including e.g. Metal Organic Framework materials (MOF's), [1] Covalent Organic Framework materials (COF's) [2] and variety of nanostructured carbon materials.[3] Carbon materials are considered as promising candidates for the storage of hydrogen using both physisorption and chemisorption [4, 5]. For example, hydrogen storage properties are well known by now for activated carbons[6],[7], carbon nanotubes [8],[9],[10]graphite nanofibers [11] and carbide derived carbons [12]. Advantage of nanostructured carbon materials is high surface area, stability and possibilities of large scale production. The main disadvantage is relatively low hydrogen storage capacity at ambient temperatures provided by physisorption.

Physisorption of hydrogen is the most attractive method for hydrogen storage due to full reversibility and simple gas loading/release procedure. Hydrogen in this case is adsorbed in molecular form and desorbed once the pressure is released. Therefore, the amount of stored hydrogen is related to surface excess and correlates with surface area. The specific surface area (SSA) is usually determined using analysis of nitrogen sorption isotherms. A material that stores hydrogen by physisorption can be added to standard H<sub>2</sub> vessels to provide additional storage capacity compared to the same volume filled with only hydrogen gas. General trends in H<sub>2</sub> physisorption are now reliably established for major types of porous materials, including many carbon materials, both at ambient temperature and at 77K. The standard trend for temperatures near ambient and pressures about 120bar is ~ 0.3wt% per 1000m<sup>2</sup>/g of BET SSA. Maximal sorption at these conditions is about 1wt% and even at much higher pressures of 300bar do not reach 2wt% [13]. This trend, sometimes called the “Chahine rule”, [6, 14] is valid for any type of carbon materials that store hydrogen by physisorption [15-17]. Similar trend is also observed for most of porous materials with high surface areas, e.g. metal-organic frameworks (MOF's) [18, 19].

It needs to be noted that hydrogen storage values reported for new materials over the past 15 years have often been overestimated in first reports [20],[21] only to settle with “standard” trend after few years of studies. Possible reasons behind irreproducibility of results in the hydrogen storage field and possible sources for measurement related errors in hydrogen sorption were recently reviewed by Broom and Hirscher.[22] In particular, the most popular volumetric method of hydrogen sorption measurements is especially sensitive to various technical issues which might lead to overestimation of hydrogen uptakes.

Most recent example of controversy is the exceptionally high hydrogen storage reported for “graphene” materials, mostly produced by reduction of graphite/graphene oxides.[23-31] In many of these studies H<sub>2</sub> sorption was reported for single sample and using only one sorption isotherm, without analysis of reproducibility of sorption in several cycles. Theoretical studies do not predict exceptional H<sub>2</sub> sorption for graphene by physisorption relative to other carbon materials with comparable SSA. In agreement with theory, our recent experiments demonstrated that hydrogen sorption by r-GO and KOH activated r-GO (a-r-GO) follows standard trends and correlates with SSA values (~100-3300 m<sup>2</sup>/g range in our experiments) both at room temperature and 77K.[32-34] Nevertheless, reports on extremely high hydrogen uptakes (either in absolute values or relative to reported SSA) by various types of r-GO continue to appear, [35]

outnumbering studies which find trivial uptake numbers.[36] In several cases the data presented as an evidence for exceptional hydrogen storage of graphene are represented by abnormal shapes of isotherms [35, 37] or obtained by rather uncommon measurement methods. For example, ~4.6wt% uptakes already at 40bar and ambient temperatures were measured by Kim et al using quartz microbalance method.[38] Another study reported over 8wt% hydrogen storage capacity measured by trivial TGA on air exposed samples after “loading” hydrogen at 60 bar. No control of evolved gases was presented for TGA experiments in this study and the whole weight loss was assigned to hydrogen. [39]

Several studies reported recently that decoration of “graphene” with various nanoparticles (e.g. Pt, Pd, TiO<sub>2</sub>) provides increase of hydrogen sorption by 10-500%.[28, 31, 37] In some studies the hydrogen storage values which satisfy and even exceed DOE targets have been reported for temperatures near ambient and assigned to “spillover” mechanism. For example, Parambath et al reported uptake of ~3wt% for Pd decorated material with SSA of ~470 m<sup>2</sup>/g already at 40bar H<sub>2</sub> pressure.[28] Extrapolating their pressure isotherms to common 120bar pressure and doubling surface area would result in unrealistic hydrogen storage of over 10 wt%. Hydrogen dissociation on nanoparticles followed by migration of atomic hydrogen on various high surface area supporting materials (spillover) was a subject of controversy over past 20 years with some groups consistently reporting spillover effect for almost any materials [40, 41] while other groups could not reproduce these results.[42-44] One can note that nanoparticle decorated materials are not used for hydrogen sorption applications even 15 years after the first reports of 5-6wt% hydrogen storage capacity at ambient temperatures. “Spillover materials” were never demonstrated as feasible even for prototypes of H<sub>2</sub> storage tanks despite multiple reports of reaching DOE targets. Poor reproducibility of “spillover” results was assigned either to details of decoration procedure [45] which were once described by authors as “more art than science” or experimental artefacts connected to measurements of sorption.[46]

In this study we report hydrogen storage measurements for Pt and Pd decorated r-GO which demonstrated an absence of spillover effect. However, we found some artefacts related to samples subjected to certain oxidation treatments which could easily be misinterpreted as “spillover”. Our results emphasize the need for a standard approach in presentation and reviewing H<sub>2</sub> sorption results to avoid erroneous reports.

## 2. Experimental

Precursor graphite oxide was synthesized using Hummers method and thermally exfoliated to produce reduced graphene oxide (r-GO), details provided in our earlier publications [32, 33]. For some experiments commercial samples of r-GO provided by Graphenea (Spain), thermally exfoliated GO provided by GRAnPH(Spain) were tested. Reference sample of activated carbon was purchased from ACS materials (USA). Since the typical SSA of r-GO is in the range 300-500m<sup>2</sup>/g, activation by KOH treatment was used to prepare several samples with higher surface area following procedures reported in our earlier studies. [33] The best SSA values were obtained for KOH activated r-GO (a-r-GO) produced by using a rapid thermal exfoliation treatment. However, the same activation procedure applied to r-GO provided by Graphenea resulted in negligible increase of SSA. We attribute the difference to the specific methods used for preparation of r-GO. The r-GO by Graphenea is prepared by chemical

reduction of GO which is expected to provide less defects compared to rapid thermal explosion of graphite oxide.

The Pd-graphene composite was synthesis as following:

Decoration of r-GO and a-r-GO was performed using several methods listed below and included Microwave Treatments (*mw*) and thermal treatments (*tt*) (**Table 1**).

*mw1* - 50mg of r-GO or a-r-GO powder was put into a mortar and grinded with 1ml toluene containing 5mg Bis(dibenzylideneacetone)palladium(0) or 5mg Tetraammineplatinum(II) nitrate for 10 mins. The mixture was dried in a fume hood and then transferred into a small beak and bubbled with argon for another two hours. Finally, the mixture was treated in a microwave oven for 2 mins and cooled down to room temperature under argon protection.

*mw2* - 200mg HGO and 21 mg palladium acetate [ $\text{Pd}(\text{O}_2\text{CCH}_3)_2$ ] were mixed in 20ml ethanol [ $\text{C}_2\text{H}_5\text{OH}$ ]. The mixture was steered for 3 hours under ambient conditions and then dried under vacuum. The mixture was treated in microwave oven in 3 steps under air with cooling down to ambient conditions after every step. At first step the mixture was treated for 30 seconds at 700W, while second and third steps were performed at 700W and 900W for 60 seconds each. This procedure was used following the report by Kumar et al. [35]

*tt* - 200mg eHGO and 21 mg palladium acetate [ $\text{Pd}(\text{O}_2\text{CCH}_3)_2$ ] were mixed in 20 ml ethanol [ $\text{C}_2\text{H}_5\text{OH}$ ]. The mixture was steered for 3 hours under ambient conditions and then dried under vacuum. The mixture was heated in oven at 673-773K for 20-60min under air in 1 step with cooling down at ambient conditions.

We prepared also several samples of “perforated graphene” by air annealing of r-GO and a-r-GO precursors using either rapid microwave treatment (following procedure given in ref [35]) or by heating in oven at 673-773K for 30-60 min. The weight of samples before and after the treatment was measured to control evaporation of carbon due to reaction with air and formation of gaseous reaction products. Microwave heating was found difficult to control while standard annealing procedure provided more reproducible results with respect to percent of remaining material and temperature of treatment.

The composition of decorated samples in respect to amount of Pd or Pt was determined using TGA as the weight of sample after complete oxidation of carbon by oxygen from air. TGA was done by using a Mettler Toledo TGA/DSC1 STARE System. Experiments were performed at a heating rate of 5K/min under air until the weight of sample become stable (~1173K).

The nitrogen sorption isotherms were measured using a Quantachrome Nova 1200e (Surface area & Pore size analyzer) apparatus with at liquid nitrogen temperature. Samples were degassed under vacuum at 423K for at least 12 h. The relative pressure range for the calculation of (BET) specific surface area was determined by plotting the adsorption isotherm as  $V(1-P/P_0)=f(P/P_0)$ . [47] The selected relative pressure range should correspond to the part for which  $V(1-P/P_0)$  continuously increases with  $P/P_0$ . [48] A QSDFT slit pore model was used to evaluate the cumulative surface area, pore volume and pore size distribution.

Hydrogen adsorption was measured at room temperature using a Rubotherm gravimetric system, see details elsewhere. [49] Precision of weight measurement using the balance is  $\pm 0.01$  mg and temperature controlled with 0.1K precision. The measurement procedure includes “zero-point correction” applied every 2 minutes which allows excluding systematic errors due to drifts.

Isotherms were recorded under H<sub>2</sub> pressures up to 120bar with typical sample size of 100-300 mg. Degassing of samples prior to H<sub>2</sub> tests was usually performed at high vacuum conditions at 423K for 12-16h. On every step of the hydrogen adsorption isotherm the temperature and pressure were stabilized for at least ~15 min using a circulation liquid thermostat. The precision in measured uptake values is estimated to be  $\pm 0.02\text{wt}\%$  for a typical 100 mg sample based on instrumental errors of the weight and temperature sensors. FLUIDCAL software was used for the calculations of fluid density of hydrogen and helium. Detailed analysis of error sources and methods of their accounting for similar gravimetric system can be found elsewhere.[50]

Ambient temperature and liquid nitrogen temperature H<sub>2</sub> adsorption tests were also performed using a Hiden Isochema Intelligent Manometric Instrument (IMI) [51],[52] volumetric system supplied with liquid nitrogen immersion cell. Typical sample mass used for measurements was in the range of 70-200mg. Prior to first measurement each sample was degassed at 423K for 8 hours. Skeletal volume was calculated from 8 measurements using He gas under pressure of 50bar, first two measurements were excluded from calculations. Typical isotherm was recorded for pressure interval 0.2-120 bar using 25 points, typical equilibration time on every point 5-7 min. The system was regularly checked for leaks using helium or hydrogen test at high pressures prior or after H<sub>2</sub> experiments. For example, the reference sample of activated carbon was tested using prolonged exposure to hydrogen at highest pressure point of isotherm. The highest excess uptake of 0.66 wt% was measured in this experiment at the last point of isotherm (112 bar). Prolonged exposure of the sample at this point for 200 min resulted in pressure drop which corresponds to “increase” of uptake up to 0.68 wt%. This example demonstrates that the error due to leaks in this experiment is well below 0.01 wt% considering typical equilibration time of 5 minutes.

Scanning electron microscopy (SEM) was carried out using a Carl Zeiss Merlin Field Emission Scanning Electron Microscope (FESEM). Accelerating voltage of 4 kV and a beam current of 100 pA were used for measurements.

### 3. Results

#### *3.1 Hydrogen sorption by r-GO and activated r-GO decorated with Pd and Pt nanoparticles.*

Results of hydrogen sorption experiments with Pd and Pt decorated samples are summarized in the **Table 1**. Enhancement of hydrogen storage was not found, independently on the type of used support materials (r-GO and a-r-GO), methods of decoration (two different metal precursors subjected to either microwave or thermal pyrolysis), size of metal nanoparticles, variation of Pd load, SSA values and additional activation treatments (hydrogen annealing).

Samples prepared for H<sub>2</sub> sorption experiments were characterized using SEM which demonstrated rather homogeneous distribution of nanoparticles over the surface of r-GO for some of studied samples (No. 2, 7, 11 from **Table 1** shown on **Figures 1, 2 and 3**). Depending on details of synthesis the size of nanoparticles varied from sample to sample in the range 3 nm-100 nm and metal loading of 4-10%. First set of experiments was performed using r-GO decorated with Pd nanoparticles and showed no increase compared to reference r-GO. Hydrogen uptakes recorded both at 295K and 77K followed standard trends in correlation with SSA values given by analysis of nitrogen sorption isotherms (**Table 1**). Therefore, some samples were

subjected to additional treatments. First, we tested high temperature annealing in hydrogen gas which allows to decrease residual oxygen content to  $\sim C/O=35$  and to remove possible contamination with oxygen and carbon from Pd nanoparticles. However, hydrogen uptake by hydrogen annealed sample was even slightly lower compared to untreated r-GO (**Figure 1**).

Samples of r-GO obtained by rapid insertion into hot furnace (as in ref. [35]) and by microwave exfoliation have not showed significant difference after decoration with Pd and exhibited similar hydrogen storage properties. Additionally, we tested as precursor r-GO prepared by chemical reduction of graphene oxide (Graphenea) and have not found any significant difference with samples prepared using thermal or microwave exfoliation.

Second set of samples was prepared using decoration of KOH activated r-GO. Experiments with a-r-GO decorated with Pt and Pd nanoparticles also did not reveal enhanced hydrogen storage. **Figure 2** shows  $H_2$  isotherms recorded for sample of a-r-GO (No. 7 in the **Table 1**) with SSA of  $2139\text{m}^2/\text{g}$  (after decoration) and Pt loading 4%. SEM characterization showed that the surface of a-r-GO is covered by rather uniformly distributed Pt nanoparticles with size 5-10nm. Hydrogen sorption of  $\sim 0.6\text{wt}\%$  at 120bar measured for this sample is in good agreement with the value expected according to standard wt% vs SSA trend. Similarly to experiments with r-GO described above, hydrogen annealing of this sample did not result in any increase of  $H_2$  sorption wt%. SEM images recorded after hydrogen annealing (**Figure 2c**) showed that nanoparticles were not anymore found on the outer surface of a-r-GO flakes. The surface of a-r-GO flakes shown in this image is covered by holes with typical size similar to the size of nanoparticles observed prior to annealing. It can be concluded that the carbon support was etched by hydrogen under and in the vicinity of the nanoparticles. Therefore, hydrogen annealing can be used for making holes in graphene by annealing at high temperatures (673K). However, no enhancement of  $H_2$  storage properties was observed for any of the decorated r-GO or a-r-GO samples neither in pristine state nor after hydrogen annealing. As reference sample of activated carbon sample was decorated with Pd nanoparticles and etched in air by microwave treatment using the same procedures (sample 9 in the **Table 1**). All samples showed  $H_2$  uptakes in reasonable agreement with values expected from known trends in wt% vs BET SSA reported in our earlier studies.

### *3.2 Effect of air etching on surface area of r-GO and a-r-GO*

Next set of experiments was performed with decorated r-GO samples aiming on preparation of “perforated graphene”. Air-etched holey r-GO samples were reported earlier to show 5-fold increase of hydrogen sorption at 77K with a rather unusual shape of isotherms. [35] Our experiments confirmed that oxygen from air is etching the carbon support around Pt or Pd nanoparticles at high temperatures thus providing formation of holes in r-GO sheets.

According to theoretical modelling, the surface area of highly defective graphene perforated with nanosized holes and arranged into 3D structures can be increased above the limit of ideal graphene ( $2650\text{m}^2/\text{g}$ ) reaching values above  $4000\text{m}^2/\text{g}$ . Surface areas above  $3000\text{m}^2/\text{g}$  have been reported in several earlier studies for various nanostructured carbon materials (up to  $\sim 3800\text{m}^2/\text{g}$ ) [53-57] and up to  $\sim 3300\text{m}^2/\text{g}$  for graphene-related materials.[33] The nanoparticle assisted methods of making holes in graphene is of interest as a possible method for further

increase SSA of graphene-related materials. Imaging using SEM confirms formation of holes around Pd nanoparticles (sample 2 in the **Table 1** shown on **Figure 3**) as a result of air etching. Moreover, increase of BET SSA by 10-30% was observed for several samples as a result of air annealing (samples 1 and 4 in the **Table 1**). However this increase was observed only for r-GO samples which typically exhibit moderate values of SSA ( $300\text{-}350\text{m}^2/\text{g}$  in these experiments) thus providing only minor overall improvement.

On the contrary, air etching tests of Pd decorated a-r-GO samples (which typically exhibit much higher SSA values) resulted in significant decrease of surface area. For example air annealing of a-r-GO with SSA of  $2448\text{m}^2/\text{g}$  at 773K for 40 minutes resulted in decrease to  $1441\text{m}^2/\text{g}$  (7% Pd). Similar treatment for 20 minutes resulted in decrease of SSA for another sample from  $1245\text{m}^2/\text{g}$  to  $466\text{m}^2/\text{g}$  (14wt% of Pd).

This result can be understood taking into account that a-r-GO has a three-dimensional structure composed of rather defective graphene flakes and an essentially nanoporous nature, while precursor r-GO consist of micrometer sized flakes. Etching of r-GO flakes will result in formation of 5-10nm holes thus providing increase of SSA values. Exceptionally high surface area of a-r-GO is due to 1-2nm size of pores and 3D architecture of defect graphene flakes.[33] Therefore, etching this structure with 5-10nm large nanoparticles is not expected to result in better porosity. In fact, air etching of a-r-GO does not result in significant change of pore size distribution as illustrated for samples 4 and 5 by **Figure 4**. Since the size of holes created by air etching must be larger relative to the size of metal nanoparticles, it is logical to expect that the 3D structure will be damaged and the SSA values will be lowered.

### *3.3 Hydrogen sorption by air etched samples: artefacts and hydrogen storage.*

Hydrogen storage parameters of selected air etched samples were characterized both at 77K and room temperatures (**Table 1**). Hydrogen sorption isotherms recorded from Pd decorated and air etched r-GO sample (No.4 in the **Table 1**) are shown in **Figure 5**. The first isotherm (recorded after vacuum degassing of sample at 423K) demonstrated unusually high wt% value relative to SSA of  $435\text{m}^2/\text{g}$ . The value of 0.45wt% is twice times higher compared to hydrogen sorption found for precursor r-GO sample and cannot be explained only by SSA increase observed after air etching treatment (~10%). Rather unusual is also the sharp step in the  $\text{H}_2$  sorption at rather low pressures, a value of ~0.25wt% is achieved already at 1bar  $\text{H}_2$  pressure.

At first glance, this isotherm could be mistakenly interpreted as an evidence of “spillover” effect and enhancement of  $\text{H}_2$  sorption by decoration of r-GO with Pd nanoparticles. However, more detailed analysis and experiments reveal that this isotherm must be considered as a measurement artefact not connected to true hydrogen storage parameters of the system, but related to chemical reaction of hydrogen with some unstable carbon or oxygen species formed in the sample as a result of air etching. **Figure 4** shows that second, third and fourth isotherms recorded from the same sample show progressively smaller values of  $\text{H}_2$  uptakes, while the shape of isotherm is closer and closer to the standard one observed for physisorption on r-GO. The difference between isotherms 1-4 is only at the first step which occurs at low pressures below 1bar. Similar step-like increase was reported earlier for other carbon materials and attributed to chemisorption of hydrogen.[58, 59] Excluding the initial step in hydrogen uptakes (contribution



from chemisorption), the remaining part of isotherm follows standard shapes and reversible hydrogen uptake expected for given SSA values. Thus, the first isotherm cannot be used to evaluate hydrogen storage parameters of this sample and needs to be considered as a measurement artefact. By definition, hydrogen storage value is amount of hydrogen which can be reversibly sorbed/desorbed by the material.

The chemisorption effect can only partly be explained by formation of palladium hydride as shown on **Figure 6** for sample 4. Since the Pd loading was relatively low (9% for given sample) formation of palladium hydride corresponds to maximum of ~0.05wt% of hydrogen storage capacity.

Evidence of chemisorption of hydrogen by air-etched r-GO samples was confirmed also using gravimetric method (**Figure 6**). In agreement with data obtained by the volumetric method, the hydrogen sorption shows step like increase on the first point of measurement and standard shape of the isotherm at higher pressures. The second cycle of hydrogen loading showed twice lower sorption. The advantage of gravimetric method is that it allows control of sample weight before and after hydrogen sorption-desorption cycle. If all technical artefacts (e.g. errors in buoyancy correction) are carefully excluded, increase of final weight can be assigned to hydrogen reaction with a sample. Irreversible weight increase should be assigned to formation of covalent C-H bonds e.g. due to hydrogenation of some carbon atoms. The decrease of total sample weight can be assigned to formation of volatile products which are evaporated from the sample under degassing conditions. For example hydrocarbons or water can possibly be produced as a result of reaction between unstable carbon or oxygen species formed in the sample after decoration with Pd nanoparticles and air annealing. The effect of chemisorption and evaporation of gaseous reaction products is rather obvious in gravimetric experiments but easy to overlook if only automated volumetric measurements are used to record isotherms. The automatic volumetric system would reset each new isotherm to zero point, while the minor volume/weight loss after final degassing would be very difficult to detect. Our experiments with hydrogen sorption by r-GO and Pd decorated r-GO have not revealed effects related to total weight increase (e.g. due to formation of C-H bonds). However, air annealed Pd decorated and air etched r-GO does demonstrate weight loss below the initial value when degassed after hydrogen loading cycles. The air annealing leads to formation of holes in r-GO flakes and other defects due to effects of oxygen etching. Therefore, it is natural to expect that air etched samples are more reactive towards hydrogen due to presence of various oxygen terminated defects.

#### 4. Discussion

Summarizing our results, samples of r-GO prepared by microwave exfoliation and by thermal exfoliation of HGO were decorated with Pd and Pt nanoparticles. The metal decorated samples were then additionally activated using either hydrogen annealing or air etching. Increase of surface area by 10-30% was observed as a result of air-etching of Pd decorated r-GO and attributed to formation of holes around metal nanoparticles. Samples of KOH activated r-GO with SSA over 1500 m<sup>2</sup>/g were also decorated with Pd and Pt nanoparticles. Hydrogen storage parameters of all above mentioned samples were studied using volumetric and gravimetric methods. None of the samples exhibited clear effects of H<sub>2</sub> storage enhancement due to addition of Pd or Pt nanoparticles. Hydrogen uptakes of decorated samples can be predicted using BET surface area similarly to none-decorated carbon materials (**Figure 7**). No effects which could be

assigned to “spillover” of hydrogen were observed for any of studied samples, even after additional activation by hydrogen annealing at 673K.

However, we report chemisorption effect for samples of air etched Pd-r-GO observed for first 1-2 hydrogen loading cycles which can be mistakenly attributed to “spillover” and hydrogen storage enhancement. The ability of sample to chemisorb hydrogen with formation of volatile products is partly restored if the sample is air exposed and must be related to formation of water or hydrocarbons on the surface of Pd. The true, reversible part of H<sub>2</sub> sorption follows standard for all carbon materials trends and correlates with BET surface area. Reaction of hydrogen with unstable carbon and oxygen species was earlier reported for other types of Pd nanoparticle decorated carbon samples. For example, reduction of PdO with formation of water was reported for Pd decorated templated carbons,[60] formation of water and covalent C-H due to hydrocarbons was also reported for Ru decorated carbon materials.[61]

Our results emphasize that reporting single hydrogen sorption isotherm (as presented in some earlier reports on “spillover” by decorated r-GO) is not sufficient for claims of improved hydrogen storage parameters. Hydrogen storage by definition includes both sorption and desorption which must be reversible after many cycles. Using gravimetric method one can easily compare sample weight before and after the hydrogen sorption, while the change of weight both to positive and negative direction will be clear sign of chemisorption.

Looking at the available literature on “spillover” in graphene related materials, it is most often that only one hydrogen sorption isotherm is reported, no degassing data following hydrogen loading provided and no reproducibility in several sorption/desorption cycles is presented. In several other studies the hydrogen sorption measurement methods deviate from standard and require independent verification by volumetric or gravimetric methods or better by both. Therefore, we can conclude that evidence for enhancement of hydrogen storage using decoration with nanoparticles is not yet sufficient or convincing.

### **Acknowledgements.**

This project has received funding from the European Union’s Horizon 2020 research and innovation program under grant agreement No. 696656 – GrapheneCore1. We also acknowledge the facilities and technical assistance of the Umeå Core Facility Electron Microscopy (UCEM) at the Chemical Biological Centre (KBC), Umeå University. We thank Graphenea and GRAnPH for samples of r-GO and GO provided for some experiments.

### **References.**

- [1] J.L.C. Rowsell, O.M. Yaghi, *Angew Chem Int Edit*, 44 (2005) 4670-4679.
- [2] S.S. Han, H. Furukawa, O.M. Yaghi, W.A. Goddard, *J Am Chem Soc*, 130 (2008) 11580-+.
- [3] D.P. Broom, C.J. Webb, K.E. Hurst, P.A. Parilla, T. Gennett, C.M. Brown, R. Zacharia, E. Tylianakis, E. Klontzas, G.E. Froudakis, T.A. Steriotis, P.N. Trikalitis, D.L. Anton, B. Hardy, D. Tamburello, C. Corngale, B.A. van Hassel, D. Cossement, R. Chahine, M. Hirscher, *Appl Phys a-Mater*, 122 (2016).
- [4] U. Eberle, M. Felderhoff, F. Schuth, *Angew Chem Int Edit*, 48 (2009) 6608-6630.
- [5] V. Tozzini, V. Pellegrini, *Phys Chem Chem Phys*, 15 (2013) 80-89.
- [6] B. Panella, M. Hirscher, S. Roth, *Carbon*, 43 (2005) 2209-2214.
- [7] H.L. Wang, Q.M. Gao, J. Hu, *J Am Chem Soc*, 131 (2009) 7016-7022.

- [8] M. Hirscher, M. Becher, *Journal of Nanoscience and Nanotechnology*, 3 (2003) 3-17.
- [9] M. Ritschel, M. Uhlemann, O. Gutfleisch, A. Leonhardt, A. Graff, C. Taschner, J. Fink, *Applied Physics Letters*, 80 (2002) 2985-2987.
- [10] B. Assfour, S. Leoni, G. Seifert, I.A. Baburin, *Adv Mater*, 23 (2011) 1237-+.
- [11] H.G. Schimmel, G.J. Kearley, M.G. Nijkamp, C.T. Visserl, K.P. de Jong, F.M. Mulder, *Chem-Eur J*, 9 (2003) 4764-4770.
- [12] G. Yushin, R. Dash, J. Jagiello, J.E. Fischer, Y. Gogotsi, *Adv Funct Mater*, 16 (2006) 2288-2293.
- [13] N.P. Stadie, J.J. Vajo, R.W. Cumberland, A.A. Wilson, C.C. Ahn, B. Fultz, *Langmuir*, 28 (2012) 10057-10063.
- [14] E. Poirier, R. Chahine, T.K. Bose, *International Journal of Hydrogen Energy*, 26 (2001) 831-835.
- [15] H. Nishihara, P.X. Hou, L.X. Li, M. Ito, M. Uchiyama, T. Kaburagi, A. Ikura, J. Katamura, T. Kawarada, K. Mizuuchi, T. Kyotani, *Journal of Physical Chemistry C*, 113 (2009) 3189-3196.
- [16] M. Becher, M. Haluska, M. Hirscher, A. Quintel, V. Skakalova, U. Dettlaff-Weglikovska, X. Chen, M. Hulman, Y. Choi, S. Roth, V. Meregalli, M. Parrinello, R. Strobel, L. Jorissen, M.M. Kappes, J. Fink, A. Zuttel, I. Stepanek, P. Bernierg, *Comptes Rendus Physique*, 4 (2003) 1055-1062.
- [17] E. Poirier, R. Chahine, P. Benard, D. Cossement, L. Lafi, E. Melancon, T.K. Bose, S. Desilets, *Applied Physics a-Materials Science & Processing*, 78 (2004) 961-967.
- [18] B. Panella, M. Hirscher, *Advanced Materials*, 17 (2005) 538-541.
- [19] S.M. Luzan, H. Jung, H. Chun, A.V. Talyzin, *International Journal of Hydrogen Energy*, 34 (2009) 9754-9759.
- [20] A.C. Dillon, K.M. Jones, T.A. Bekkedahl, C.H. Kiang, D.S. Bethune, M.J. Heben, *Nature*, 386 (1997) 377-379.
- [21] N.L. Rosi, J. Eckert, M. Eddaoudi, D.T. Vodak, J. Kim, M. O'Keeffe, O.M. Yaghi, *Science*, 300 (2003) 1127-1129.
- [22] D.P. Broom, M. Hirscher, *Energ Environ Sci*, 9 (2016) 3368-3380.
- [23] A. Ghosh, K.S. Subrahmanyam, K.S. Krishna, S. Datta, A. Govindaraj, S.K. Pati, C.N.R. Rao, *J Phys Chem C*, 112 (2008) 15704-15707.
- [24] K.S. Subrahmanyam, S.R.C. Vivekchand, A. Govindaraj, C.N.R. Rao, *Journal of Materials Chemistry*, 18 (2008) 1517-1523.
- [25] G. Srinivas, Y.W. Zhu, R. Piner, N. Skipper, M. Ellerby, R. Ruoff, *Carbon*, 48 (2010) 630-635.
- [26] L.F. Wang, N.R. Stuckert, R.T. Yang, *Aiche Journal*, 57 (2011) 2902-2908.
- [27] W.H. Yuan, B.Q. Li, L. Li, *Appl Surf Sci*, 257 (2011) 10183-10187.
- [28] V.B. Parambath, R. Nagar, K. Sethupathi, S. Ramaprabhu, *J Phys Chem C*, 115 (2011) 15679-15685.
- [29] L.P. Ma, Z.S. Wu, J. Li, E.D. Wu, W.C. Ren, H.M. Cheng, *Int J Hydrogen Energy*, 34 (2009) 2329-2332.
- [30] C.X. Guo, Y. Wang, C.M. Li, *Acs Sustain Chem Eng*, 1 (2013) 14-18.
- [31] V.B. Parambath, R. Nagar, S. Ramaprabhu, *Langmuir*, 28 (2012) 7826-7833.
- [32] A.G. Klechikov, G. Mercier, P. Merino, S. Blanco, C. Merino, A.V. Talyzin, *Micropor Mesopor Mat*, 210 (2015) 46-51.
- [33] A. Klechikov, G. Mercier, T. Sharifi, I.A. Baburin, G. Seifert, A.V. Talyzin, *Chem Commun*, 51 (2015) 15280-15283.
- [34] I.A. Baburin, A. Klechikou, G. Mercier, A. Talyzin, G. Seifert, *Int J Hydrogen Energ*, 40 (2015) 6594-6599.
- [35] R. Kumar, J.H. Oh, H.J. Kim, J.H. Jung, C.H. Jung, W.G. Hong, H.J. Kim, J.Y. Park, I.K. Oh, *Acs Nano*, 9 (2015) 7343-7351.
- [36] A. Ganesan, M.M. Shaijumon, *Micropor Mesopor Mat*, 220 (2016) 21-27.
- [37] H. Jung, K.T. Park, M.N. Gueye, S.H. So, C.R. Park, *Int J Hydrogen Energy*, 41 (2016) 5019-5027.
- [38] T.H. Kim, J. Bae, T.H. Lee, J. Hwang, J.H. Jung, J.S. Lee, D.O. Kim, Y.H. Lee, J. Ihm, *Nano Energy*, 27 (2016) 402-411.

- [39] C.Z. Zhou, J.A. Szpunar, *Applied materials and Interfaces*, early view (2016).
- [40] A. Lueking, R.T. Yang, *J Catal*, 211 (2002) 565-565.
- [41] Y.W. Li, R.T. Yang, *J Am Chem Soc*, 128 (2006) 726-727.
- [42] R. Campesi, F. Cuevas, M. Latroche, M. Hirscher, *Phys Chem Chem Phys*, 12 (2010) 10457-10459.
- [43] S.M. Luzan, A.V. Talyzin, *Micropor Mesopor Mat*, 135 (2010) 201-205.
- [44] N.P. Stadie, J.J. Purewal, C.C. Ahn, B. Fultz, *Langmuir*, 26 (2010) 15481-15485.
- [45] N.R. Stuckert, L.F. Wang, R.T. Yang, *Langmuir*, 26 (2010) 11963-11971.
- [46] R. Prins, *Chem Rev*, 112 (2012) 2714-2738.
- [47] M. Thommes, K. Kaneko, A.V. Neimark, J.P. Olivier, F. Rodriguez-Reinoso, J. Rouquerol, K.S.W. Sing, *Pure Appl Chem*, 87 (2015) 1051-1069.
- [48] J. Rouquerol, P. Llewellyn, F. Rouquerol, *Characterization of Porous Solids VII - Proceedings of the 7th International Symposium on the Characterization of Porous Solids (Cops-Vii)*, Aix-En-Provence, France, 26-28 May 2005, 160 (2006) 49-56.
- [49] A.V. Talyzin, A. Jacob, *Journal of Alloys and Compounds*, 395 (2005) 154-158.
- [50] G. De Weireld, M. Frere, R. Jadot, *Measurement Science & Technology*, 10 (1999) 117-126.
- [51] M.D. Dolan, K.G. McLennan, D. Chandra, M.A. Kochanek, G. Song, *J Alloy Compd*, 586 (2014) 385-391.
- [52] J. Srenscek-Nazzal, W. Kaminska, B. Michalkiewicz, Z.C. Koren, *Industrial Crops and Products*, 47 (2013) 153-159.
- [53] M. Jorda-Beneyto, F. Suarez-Garcia, D. Lozano-Castello, D. Cazorla-Amoros, A. Linares-Solano, *Carbon*, 45 (2007) 293-303.
- [54] Y.D. Xia, G.S. Walker, D.M. Grant, R. Mokaya, *J Am Chem Soc*, 131 (2009) 16493-16499.
- [55] H.L. Jiang, B. Liu, Y.Q. Lan, K. Kuratani, T. Akita, H. Shioyama, F.Q. Zong, Q. Xu, *J Am Chem Soc*, 133 (2011) 11854-11857.
- [56] Z.X. Ma, T. Kyotani, A. Tomita, *Carbon*, 40 (2002) 2367-2374.
- [57] L. Zhang, F. Zhang, X. Yang, G.K. Long, Y.P. Wu, T.F. Zhang, K. Leng, Y. Huang, Y.F. Ma, A. Yu, Y.S. Chen, *Scientific Reports*, 3 (2013).
- [58] S.B. Kalidindi, H. Oh, M. Hirscher, D. Esken, C. Wiktor, S. Turner, G. Tendeloo, R.A. Fischer, *Chem-Eur J*, 18 (2012) 10848-10856.
- [59] H. Oh, T. Gennett, P. Atanassov, M. Kurttepelis, S. Bals, K.E. Hurst, M. Hirscher, *Micropor Mesopor Mat*, 177 (2013) 66-74.
- [60] C.M. Ghimbeu, C. Zlotea, R. Gadiou, F. Cuevas, E. Leroy, M. Latroche, C. Vix-Guterl, *J Mater Chem*, 21 (2011) 17765-17775.
- [61] J.L. Blackburn, C. Engtrakul, J.B. Bult, K. Hurst, Y.F. Zhao, Q. Xu, P.A. Parilla, L.J. Simpson, J.D.R. Rocha, M.R. Hudson, C.M. Brown, T. Gennett, *J Phys Chem C*, 116 (2012) 26744-26755.

TABLES

#No	Decoration method and conditions	Precursor	BET (m <sup>2</sup> /g) / Relative pressure (P/P <sub>0</sub> )		Max (and reversible) excess uptake, RT at 120bar (wt%)	Max uptake 77K at ~45bar (wt%)	Metal load (wt%)
			SSA before decoration	SSA after decoration			
1	<b>tt</b> /673K/60 min	r-GO	339 / 0.1-0.3	350 / 0.08-0.1	-	-	8
2	<b>tt</b> /773K/30 min	r-GO	339 / 0.1-0.3	320 / 0.08-0.1	0.55 (0.31)	1.29	9
3	<b>tt</b> /723K/30 min	r-GO	339 / 0.1-0.3	325 / 0.08-0.1	-	-	7
4	<b>tt</b> /773K/60 min	r-GO	339 / 0.1-0.3	435 / 0.07-0.09	0.46 (0.23)	1.07	9
5	<b>tt</b> /773K/60 min	r-GO (GRAnPH)	204 / 0.1-0.3	178 / 0.1-0.21	0.28 (0.31)	-	32
7	<b>mwt1</b>	KOH activated r-GO/Pt		2139 / 0.18-0.3	0.6 (0.59)	-	4
8	<b>mwt1</b>	KOH activated r-GO		1745 / 0.18-0.3	0.53	-	4
9	<b>mwt2</b>	Activated Carbon	1870 / 0.1-0.3	1480 / 0.08-0.14	0.6 (0.58)	-	10
10	<b>mwt2</b>	r-GO	339 / 0.1-0.3	319 / 0.09-0.12	0.24 (0.15)	0.82	9
11	<b>mwt2</b>	r-GO (graphenea)	463 / 0.1-0.3	403 / 0.17-0.3	0.17(0.14)	-	13

**Table 1.** Hydrogen sorption by Pd decorated r-GO based samples (except for sample N7 decorated by Pt). Samples 1-5 were prepared using thermal treatment (**tt**), samples 7-11 were prepared using microwave treatment (**mwt**).

FIGURES

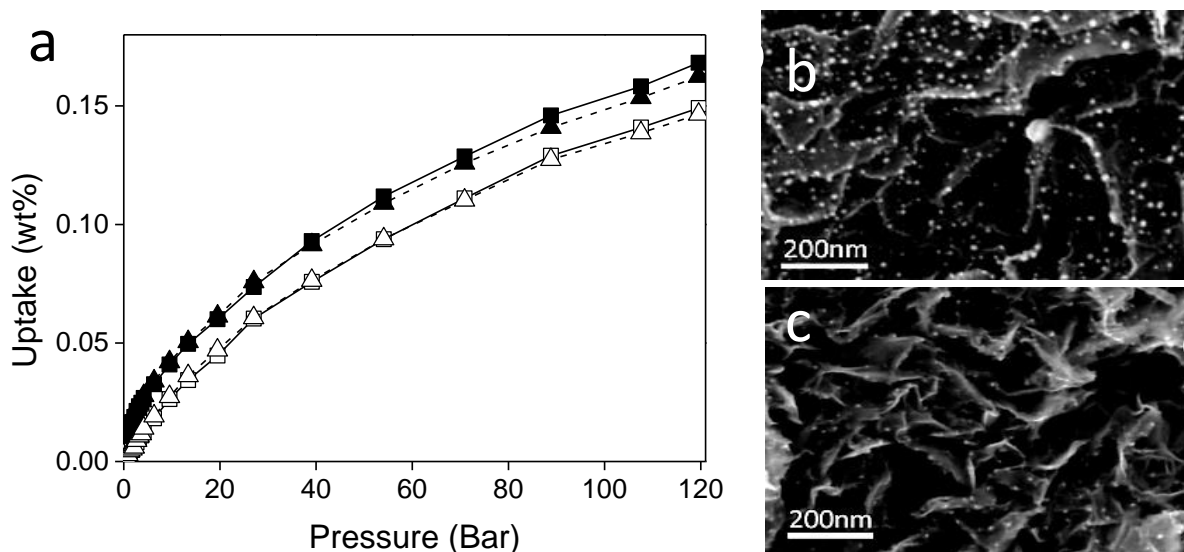


**Figure 1.** a) Hydrogen sorption isotherms recorded at 293K (excess uptake, volumetric method) for sample of r-GO decorated with Pd nanoparticles (sample 11 in the **Table 1**) The sample was degassed under vacuum at 423K for 10 hours prior hydrogen loading for cycle 1 isotherm (■). Second isotherm (□) was recorded after 5 min vacuum degassing at ambient temperature. After vacuum degassing the sample was *in situ* annealed at 623K under 50bar of H<sub>2</sub>. Hydrogen sorption isotherms from the hydrogen annealed sample were recorded without exposure of sample to air: cycle 1 (▲) after degassing at 423K for 10 hours and cycle 2 (△) after 5 min vacuum degassing. The data demonstrate that hydrogen annealing have not changed sorption properties of Pd decorated r-GO sample. b), c)- SEM images recorded from the same sample after hydrogen sorption tests demonstrating homogeneous distribution of Pd nanoparticles over the carbon support

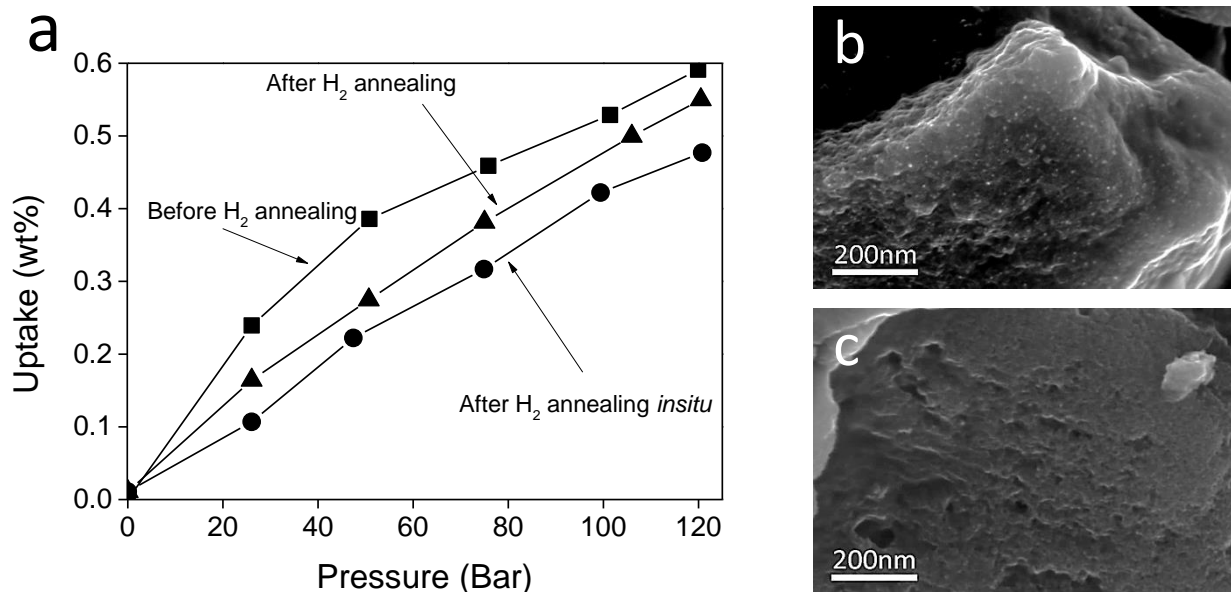


**Figure 2.** a) Hydrogen sorption isotherms (excess uptake, gravimetric method) for Pt decorated (SSA=2139m<sup>2</sup>/g) sample (No. 7 in the **Table 1**): recorded from pristine sample (■); the same sample annealed at 673K under hydrogen (50bar) *ex situ*, air exposed (▲); recorded from the same sample hydrogen annealed at 673K *in situ* without air exposure. Sample was degassed under vacuum at 423K prior to recording all three isotherms. b) SEM images recorded from the sample after decoration with Pt nanoparticles and c) after H<sub>2</sub> annealing which resulted in etching of carbon support and format ion of holes.

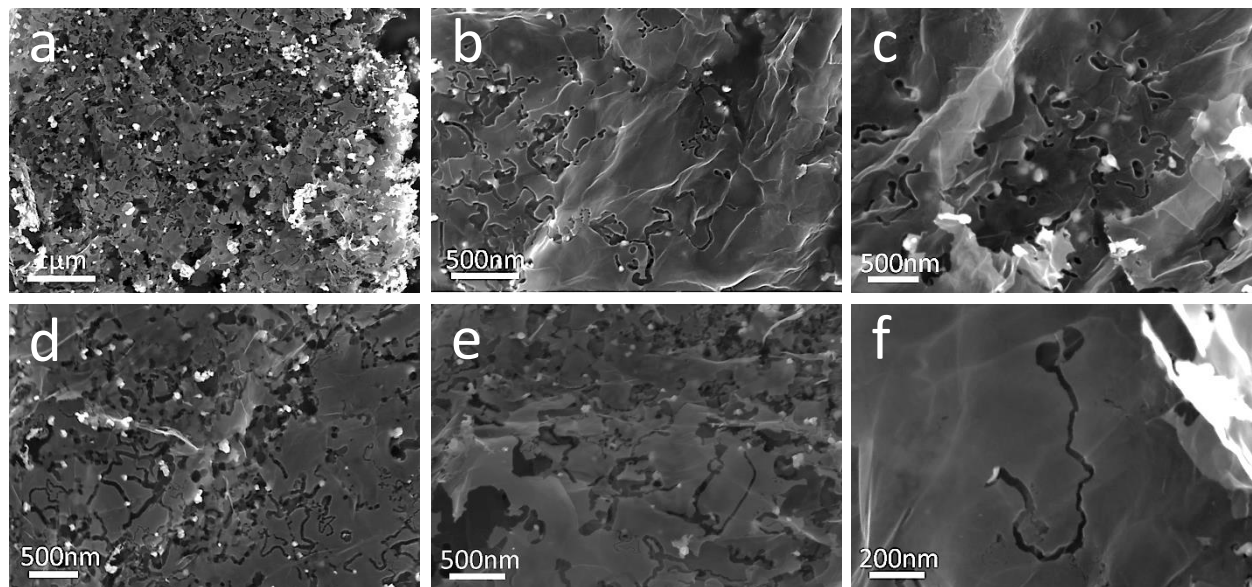


**Figure 3.** SEM images recorded from Pd decorated r-GO (sample 2, **Table 1**). Air etching results in formation of holes around the particles and worm-like traces.

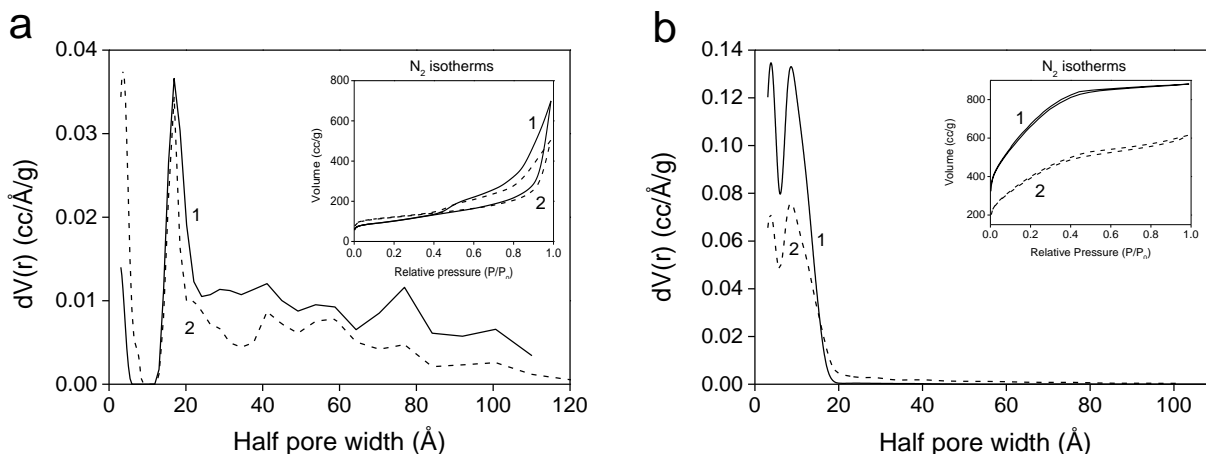


**Figure 4.** Pore volume distribution plot prepared using analysis  $N_2$  isotherms (shown as inset) by QSDFT slit pore model: a) Pd decorated r-GO (sample 4 in the **Table 1**) (1) and its r-GO precursor (2), b) Pd decorated a-r-GO (Sample 5 in the **Table 1**) (1) and its a-r-GO precursor (2).

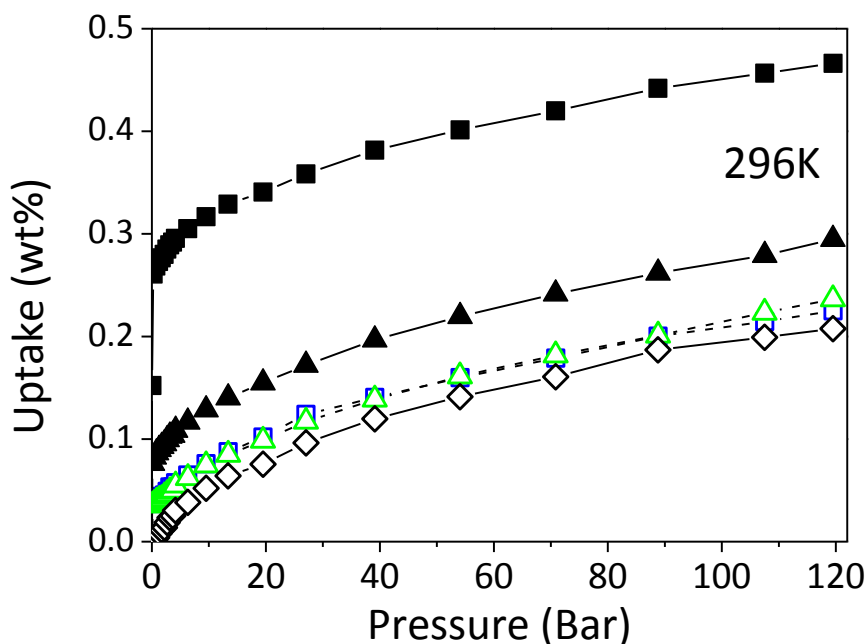


**Figure 5.** a) Hydrogen sorption isotherms (excess uptake, volumetric method) recorded from Pd decorated r-GO sample subjected to air annealing at 773K for 60 min (Sample 4 in **Table 1**). Prior to first cycle (■) the sample was degassed at 423K for 10 hours; second cycle (□) was recorded after hydrogen pressure release and 5 min vacuum degassing. On the next step the sample was degassed at vacuum conditions for 10 hours at 423K and hydrogen isotherm for cycle 3 recorded (▲); hydrogen pressure was released and cycle 4 isotherm (△) recorded after 5 min degassing at vacuum conditions (296K). Isotherm recorded for precursor r-GO sample is shown as reference (◇).



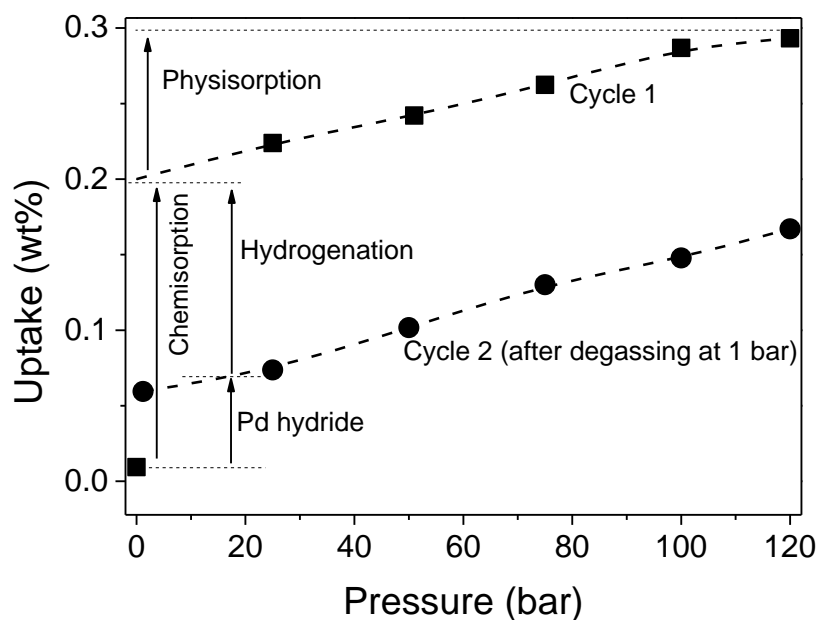


**Figure 6.** Excess H<sub>2</sub> uptakes measured for samples of Pd decorated and air annealed r-GO using gravimetric method (same sample as in Figure 5). The sample was degassed at 423K prior to cycle 1 isotherm. Hydrogen pressure was then decreased from 120bar to 1bar. After 25 minutes at 1bar the H<sub>2</sub> pressure was increased again to 120bar (cycle 2). Similar experiment where only physisorption effect is observed, the Cycle 2 isotherm would repeat exactly the Cycle 1 isotherm. The final weight of sample after hydrogen pressure release decreased by 0.2% compared to initial weight recorded after vacuum degassing of the sample.

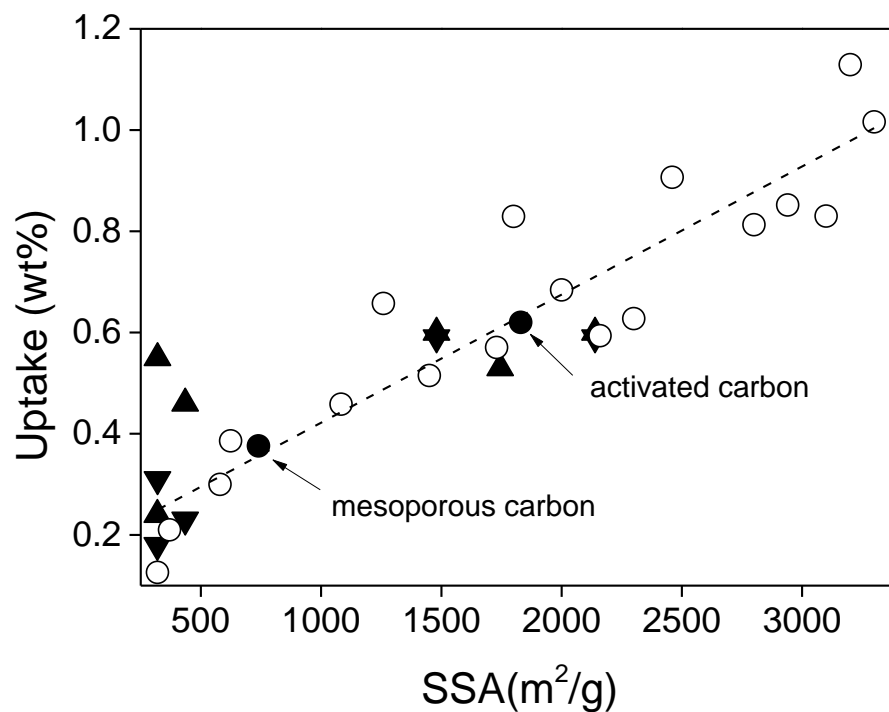


**Figure 7.** H<sub>2</sub> uptake (excess wt%) vs SSA trends evaluated using volumetric method for Pd/Pt decorated samples at 296K and 120bar: (▲)- first cycle and (▼) – second cycle. Reference trend provided by nanoparticle-free r-GO and a-r-GO samples (○), including data points from earlier published studies [32, 33] and reference points for activated carbon and mesoporous carbon (●).